NASA
Technical Memorandum 106101

AVSCOM
Technical Report 92–C–009

IN-37
169435
P.16

Face-Gear Drives: Design, Analysis, and Testing for Helicopter Transmission Applications

F.L. Litvin and J.-C. Wang
University of Illinois at Chicago
Chicago, Illinois

R.B. Bossler, Jr.
Lucas Western, Inc.
City of Industry, California

Y.-J.D. Chen and G. Heath
McDonnell Douglas Helicopter Co.
Mesa, Arizona

and

D.G. Lewicki
Propulsion Directorate
U.S. Army Aviation Systems Command
Lewis Research Center
Cleveland, Ohio

Prepared for the American Gear Manufacturers Association
1992 Fall Technical Meeting
sponsored by the American Gear Manufacturers Association
Baltimore, Maryland, October 26–28, 1992

NASA

US ARMY
AVIATION
SYSTEMS COMMAND

FACE-GEAR DRIVES: DESIGN, ANALYSIS, AND TESTING FOR HELICOPTER TRANSMISSION APPLICATIONS

F.L. Litvin and J.-C. Wang
University of Illinois at Chicago
Chicago, Illinois 60680

R.B. Bossler, Jr.
Lucas Western, Incorporated
City of Industry, California 91749

Y.-J.D. Chen and G. Heath
McDonnell Douglas Helicopter Company
Mesa, Arizona 85205

and

D.G. Lewicki
Propulsion Directorate
U.S. Army Aviation Systems Command
Lewis Research Center
Cleveland, Ohio 44135

SUMMARY

The use of face-gears in helicopter transmissions was explored. A lightweight, split-torque transmission design utilizing face-gears is described. Face-gear design and geometry were investigated. Topics included tooth generation, limiting inner and outer radii, tooth contact analysis, contact ratio, gear eccentricity, grinding, and structural stiffness. Design charts were developed to determine minimum and maximum face-gear inner and outer radii. An analytical study showed that the face-gear drive is relatively insensitive to gear misalignment with respect to transmission errors, but the tooth contact is affected by misalignment. A method of localizing the bearing contact to permit operation with misalignment was explored. Two new methods for grinding of the face-gear tooth surfaces were also investigated. The proper choice of shaft stiffness enabled good load sharing in the split-torque transmission design. Face-gear experimental studies were also conducted. These tests demonstrated the feasibility of face-gears in high-speed, high-load applications such as helicopter transmissions.

INTRODUCTION

The Advanced Rotorcraft Transmission (ART) program is an Army funded, joint Army/NASA program to develop and demonstrate lightweight, quiet, durable drivetrain systems for next generation rotorcraft (ref. 1). One contract team participant, McDonnell Douglas Helicopter Co. (MDHC)/Lucas Western Inc., developed a novel split torque ART configuration using face-gears (refs. 2 and 3). The geometry and design of face-gears and computerized simulation of their meshing have been developed by another member of the team, the University of Illinois at Chicago.

Manufacturing of face-gears was proposed many years ago by the Fellows Corporation. Face-gears have had widespread use in low power applications (fig. 1) but have not had much development for design and manufacturing practices necessary for high power use.

The theory of face-gear drives has not been developed sufficiently for the needs of the designers and manufacturers. Publications in this area in English by E. Buckingham (ref. 4) and D.W. Dudley (ref. 5) can be considered only as a brief description of face-gear drives. J. Davidov (ref. 6), and F.L. Litvin and L.J. Liburkin (ref. 7) have published the results of their investigation of face-gear drives in Russian literature, but these works are not familiar in the western world.

The advantages of face-gear drives are: (1) reduced sensitivity of the bearing contact to gear misalignment, (2) reduced level of noise due to the very low level of transmission errors, (3) more favorable conditions of transfer of load from one pair of teeth to the next pair of teeth, and (4) accurate axial location of the pinion is not required in contrast to such requirement for the spiral bevel opinions (fig. 2). Statement (3) is based on the advantage of involute gearing to have a common normal for those teeth that are finishing and starting the meshing. The analysis shows that the face-gear drives maintain the conjugate action because the face-gear teeth are generated as conjugated to the pinion teeth. The amount of misalignment that can be tolerated is easily controlled

by the manufacturing process. The comparison made was for misalignments greater than spiral bevel gears can tolerate.

The majority of the work in this paper has been presented in reference 8, with the exception of face-gear grinding investigations. This paper shows that with proper design face-gear drives can find a successful application in high power applications. The results of computerized simulation of meshing and bearing contact and experimental test of face-gear drives confirm that such drives can be successfully applied.

The paper covers application of face-gear drives in helicopter transmissions. The advantage of this design is the possibility to split the torque between two face-gear drives. This results in a significant savings in transmission weight. The design of face-gear drives, simulation of meshing and bearing contact, and grinding of the face-gear tooth surfaces, have been analytically described. Computer programs and design charts have been developed. The torque split has been confirmed by finite element structural analysis. Prototype face-gear drives have been successfully tested at NASA Lewis Research Center.

All types of gears, including face-gears, have niches where their advantages are greater than competing types. This program is an attempt to explore an application where face-gears appear to offer an advantage.

SPLIT-TORQUE DESIGN

The idea of torque split is illustrated in figure 2. Figure 2(a) shows an alternative version of the torque splitting by two spiral bevel pinions, *a* and *b*, designed as one rigid body. Figure 2(b) shows the second version of the split of torque when a single spur (or helical) pinion is in mesh with two face-gears. An advantage of the face-gear version is that the same transmitted power results in a reduced load on the bearings in comparison with the spiral bevel version shown in figure 2(a). A second advantage is that the pinion is a conventional spur (or helical) gear compared to a complex spiral bevel design with two pinions.

The general configuration of the MDHC/Lucas ART design is illustrated conceptually in figure 3. There are two engines rated at 2500 hp each which combine to drive the rotor shaft with 5000 hp. The transmission is designed to carry 3000 hp per side for a one-engine inoperative condition. Power flows from the engine through an overrunning positive-engagement clutch to a spur pinion, which is lightly restrained radially. The spur pinion drives a downward-facing face-gear and an upward-facing face-gear. The face-gear shafts terminate in spur pinions, which drive a large combining gear. The hub of the combining gear is attached to the sun gear of a high contact ratio planetary gear set where the carrier is the output member and is attached to the rotor shaft. A small pinion is driven at the aft side of the main combining gear. This pinion drives another face-gear mounted on the NOTAR™ (no tailrotor) driveshaft, which leads aft directly to a NOTAR™ fan.

The concept of torque split appears to be a significant development wherein an input spur-gear pinion drives two face-gears arranged to provide an accurate division of power. This division greatly reduces the size and weight of the corner-turning hardware as well as the size and weight of the next reduction stage. The predicted payoff is greatly reduced weight and cost compared to conventional design.

The pinion which serves the two face-gears is a conventional spur gear with an even number of teeth. If the spur gears were rigidly located between the two face-gears, precise torque splitting would be very unlikely. The spur gear has a free-floating mount which allows self-centering between the two face-gears. The effect of normal manufacturing inaccuracy on torque split will be compensated by automatic relocation of the input pinion to its balanced position as long as compliant support is provided for the front end of the pinion shaft. It will be shown analytically (see next section) that precise torque splitting (with ±1.0 percent) will take place.

More importantly, torque splitting between two driven gears by a free-floating spur-gear pinion has been used for many years in truck transmissions. The first known truck application was the experimental Road Ranger transmission produced by the Fuller Transmission Division of the Eaton Manufacturing Company in 1961. Truck transmissions using this principle have been in production since 1963. In addition to accurate torque splitting, it was found that gear noise was reduced and gear life was increased. Thus the use of a free-floating pinion as a torque-splitting device is well substantiated.

The gear chain formed by the input pinion, two face-gears, two spur pinions and the combining gear is a *closed loop locked train.* Errors of gear tooth orientation may cause a nonsatisfactory system backlash or even the impossibility to assemble the closed loop train. However, since the face-gears and the combining gear are provided with prime number teeth, indexing by assembly will enable the tooth angular orientation inside of the chain to change and provide the satisfactory system backlash. This is similar to the practice of assembly of locked trains used in marine drives. In reality, there is a need in one test assembly only. Then, the required indexing can be accomplished in accordance with the developed chart.

FINITE ELEMENT STRUCTURAL ANALYSIS FOR THE SPLIT-TORQUE GEAR DRIVE

The success of a split-torque gear-train design depends on the equal division of the torque to the two output shafts. Conceptually, the floating pinion design makes the system of the pinion shaft a

two-force member. The transmitted forces on the two diametrically opposite meshing points on the pinion have to balance each other to achieve equal torque splitting.

The analytical effort to validate the split-torque concept was conducted through use of the finite element method. To analyze the deflection and the percentage of torque splitting, the elasticity of the gear structure and pinion shaft support have to be considered first. The finite element model provides an accurate approach to include the stiffness and the deflection of the gear structure. The overall model of the split-torque gear train is shown in figure 4. This model has been used to analyze the torque-splitting percentage for different support conditions as shown in table I. The stiffness of the front and rear support of the pinion shaft were varied to determine their effect on torque split (cases 1 to 4, table I). The contacts between the pinion and the two face-gears were modeled using gap elements. The torque split was determined using gap element reaction forces as calculated using finite element analysis. Among the cases studied, the most even torque split was provided in case 9 when the stiffness of the shaft's front support was 6.0×10^4 lb/in. This is an order of magnitude less than a typical bearing support.

The use of backlash control to compensate for the difference in the tangential stiffness between the two output shafts was investigated. In reality, the exact compliance between the teeth of the three gears is not practical. The deviation from the common engagement is caused not only by the different stiffness of the two paths but also by the indexing problem associated with the closed-loop gear train design. Additional analyses have been performed to incorporate the initial clearance on any one side of the pinion to simulate unequal backlash conditions. This was done by setting an initial clearance in the appropriate gap element. The influence of unequal backlash on load sharing in the split-torque drive system is also given in table I. The effect of clearance on torque split was small but should be considered when fine-tuning a design for optimal load sharing. The analysis results are the baseline for using backlash control in assembling an equal torque-splitting drive in practice.

A structural dynamic analysis was carried out to determine a resonance free system by stiffening the fully compliant support at the front end of the pinion shaft. The selection of the pinion support with the designed spring rate to remain nearly equal torque splitting and to meet the structural dynamics criteria is the key to the design of the split-torque mechanism. When an in-plane spring rate of 6×10^4 lb/in. was designed for the input shaft front support, the first natural frequency of the shaft was 30 percent higher than the operational rotating speed. A few devices which may provide the compliance to obtain even torque splitting were studied. The torque-split mechanism must be as compliant as possible yet stiff enough to ensure the frequency of the first vibrational mode is higher than the rotating speed of the pinion shaft to avoid resonance. The current effort in design concentrates on a squirrel cage spring support and a resilient bearing mount. The design should preclude any slip of the bearing outer ring. Also, the working range of the spring should be large enough for the movement of the pinion shaft to find its new center position of balance.

The dynamic effects of the input shaft will be tested during the torque-split test. It is observed that the radial displacement of the input pinion is restricted since it is opposed by the face-gear teeth with which the pinion is in mesh. Recall that the pinion is in simultaneous mesh with two face-gears. In addition, friction that accompanies the torque transmission will cause a damping effect to resist the resonant vibration response. The small displacements that do occur will have no effect on the overrunning clutch due to the soft shaft mount and the remote location of the clutch with respect to the input pinion.

In addition to the analysis of torque splitting, the accurate rating system for the face-gear is under development using TCA and finite element method. Conservative approximation in calculating bending stresses and contact stresses has been used in the current design. The calculation shows that the strength of the face-gears is competitive to other types of gears. Moreover, the feasibility in constructing a split- torque configuration make the gear train a more compact design than the others. The risk of scoring is eliminated by localization of bearing contact. The accomplishment of a circumstantial rating system will further promote the applications of face-gears.

INFLUENCE OF GEAR ECCENTRICITY

The influence of gear eccentricity is important for determination of conditions of the split of torque when one pinion is in mesh with two face-gears, and the pinion and the gears have eccentricity. Due to transmission errors the driven face-gears will perform rotation with slightly different angular velocities, and this means that the torque split will be accompanied with deflections of tooth surfaces.

The function of transmission error is defined as,

$$\Delta\phi_2' = \phi_2' - \frac{N_1}{N_2}\left(\phi_1' - \phi_1''\right) \tag{1}$$

where N_1 and N_2 are the number of teeth of the pinion and the gear, respectively; ϕ_1' and ϕ_2' are the angles of rotation of the pinion and the gear, respectively; ϕ_1'' is the value of ϕ_1 that corresponds to $\phi_2' = 0$.

The results of investigation show that the transmission error function due to eccentricity of the pinion or the gear only is an approximate harmonic curve. The periods of these curves are the

time periods for one revolution of the pinion and the gear, respectively. The function of transmission errors for the case with eccentricity of both the pinion and the gear is a periodic one as shown in figure 5. The period of this function is determined by the lowest common multiple of the numbers of teeth of the pinion and the gear.

The great advantage of face-gear drive with an involute pinion is that the pinion teeth are equidistant and have a common normal. This means at the end of the meshing of a pair of teeth and the beginning of meshing a next pair of neighboring teeth, both tooth pairs will have a common normal. Therefore, the change of tooth meshing at the transfer point will not cause a jump of angular velocity. This statement is correct as well for eccentric conventional involute gears. This implies that noise and vibration are relatively insensitive to gear misalignment.

BASIC TOPICS OF GEAR DESIGN AND MANUFACTURING

Pitch Surfaces

In the case of bevel gears the pitch surfaces of the gears are two cones of angles γ_1 and γ_2. The cones roll over each other in the process of transformation of motions (fig. 6(a)).

In the case of a face-gear drive with intersected axes of motion the pitch surface of the pinion is the cylinder of radius r_{p1}, and the pitch surface of the face-gear is the cone of angle γ where γ is the angle of intersection (fig. 6(b)). The pitch surface of the face-gear is a plane if $\gamma = 90°$. The pitch point P is the point of intersection of the generatrix of the pinion pitch cylinder with the instantaneous axis of rotation OI. The location of point P affects the conditions of pointing and undercutting of the face-gear teeth.

Generation of Face-Gear Drives with Localized Bearing Contact

The generation of the face-gear by a shaper is shown in figure 7. The shaper and the gear rotate about intersecting axes with angular velocities $\omega^{(s)}$ and $\omega^{(2)}$ that are related as follows

$$\frac{\omega^{(s)}}{\omega^{(2)}} = \frac{N_2}{N_s} \tag{2}$$

The designations of s and 2 indicate the shaper and the face-gear, respectively.

If the face-gear is generated by a shaper that is identical to the pinion, the process of generation simulates the meshing of the pinion with the face-gear being in *line* contact at every instant. In reality, such type of contact is not useful in practice due to its sensitivity to misalignment. The errors (tolerances) of assembly and manufacturing can cause separation of the contacting surfaces and result in the undesirable contact at the edge. To avoid this, it is necessary to use a shaper with a larger number of teeth. The difference is denoted as $\Delta N = N_s - N_1$ (N_1 is the number of the pinion teeth; ΔN ranges from 1 to 3).

The geometric aspects of localization of bearing contact are illustrated with the sketch shown in figure 8. We may imagine that three surfaces – Σ_s, Σ_1, and Σ_2 – are in mesh with each other simultaneously. Surfaces Σ_s and Σ_2 are in *line* contact at every instant in the process for generation. Surfaces Σ_s and Σ_1 are also in *line* contact being in an imaginary internal engagement as shown in figure 8. The imaginary meshing of the shaper and the pinion may be considered as a meshing with the following features: (1) the center distance B depends on the difference ΔN of the number of teeth of the shaper and the pinion and (2) there is an instantaneous axis of rotation that intersects the extended center distance O_sO_1 at point P and is parallel to the axes of the pinion and the shaper.

The location of point P can be determined as the point of intersection of the common tangent to the base circles of the shaper and the pinion with the extended center distance O_sO_1 (fig. 8). PM is the common normal to the involute shapes of the shaper and the pinion.

Meshing of the Shaper, the Pinion, and the Face-Gear

The shaper tooth surface Σ_s and the face-gear tooth surface Σ_2 contact each other at every instant at a spatial line L_{s2}. Contact lines L_{s2} on the shaper tooth surface Σ_s are shown in figure 9(a). The imaginary meshing of the shaper and pinion tooth surfaces, Σ_s and Σ_1, has been illustrated with the drawings of figure 9. Surfaces Σ_s and Σ_1 contact each other at every instant at a line L_{s1}. Lines L_{s1} on surface Σ_s are shown in figure 9(b). However, the pinion tooth surface Σ_1 and the face-gear tooth surface Σ_2 contact each other at every instant at point M, that is the point of intersection of lines L_{s1} and L_{s2} (fig. 9(c)). The contact of the pinion and the face-gear surfaces under the load is a contact over an elliptical area; the center of such an ellipse is the theoretical contact point M of Σ_2 and Σ_1. The input design data for an example of a face-gear drive are given in table II. These data are used for computations demonstrated in the following sections.

Contact lines L_{s2} on the face-gear tooth surface Σ_2 are shown in figure 10. The part of the face-gear tooth surface that is not covered with lines L_{s2} is the fillet surface. The fillet surface is generated in the process of cutting by the generatrix G of the addendum cylinder of the shaper (fig. 9(a)). The fillet surface and the working part of the face-gear have a common line L^* (fig. 10).

The contact lines on Σ_s and Σ_2 are derived from the following equations (ref. 9):

1. Contact lines on the shaper surface (fig. 9 (a)) are defined as

$$r_s(u_s,\ \theta_s), \qquad N_s \cdot V_s^{(s2)} = f(u_s,\ \theta_s,\ \phi_s) = 0 \qquad (3)$$

2. Contact lines on the face-gear surface (fig. 10) are determined as

$$r_2(u_s, \theta_s, \phi_s) = [M_{2s}(\phi_s)] \quad r_s(u_s, \theta_s), \quad f(u_s, \theta_s, \phi_s) = 0 \qquad (4)$$

Here, (u_s, θ_s) are the Gaussian coordinates of the involute shaper surface (see Appendix A in ref. 10) and ϕ_s is the generalized parameter of motion.

Tooth surface Σ_2 of the face-gear is represented by equation (4) in three-parametric form with an implicit function between parameters (u_s, θ_s, ϕ_s). Fortunately, the equation of meshing

$$f(u_s, \theta_s, \phi_s) = 0 \qquad (5)$$

is linear with respect to u_s and this enables us to eliminate u_s and represent Σ_2 in two-parametric form as

$$r_2 = r_2(\theta_s, \phi_s) \qquad (6)$$

Figure 11 shows the cross-sections of the face-gear to depict the changing tooth profiles on Σ_2 and the pointing at the outside radius.

Limitations of Face-Gear Tooth Surface

The length of the tooth surface of a face-gear is limited, due to the possibility of undercutting by the shaper in the dedendum area and the pointing of the teeth in the addendum area (fig. 10).

The investigation of conditions of nonundercutting of the face-gear is based on the theorem that has been proposed by Litvin (ref. 9). The theory states that there is a *limiting* line L on the generating surface (shaper surface Σ_s) that generates *singular* points on face-gear surface Σ_2. The *limiting* line on Σ_s can be determined with the equation

$$V_r^{(s)} + V^{(s2)} = 0 \qquad (7)$$

Here; $V_r^{(s)}$ is the velocity of contact point in its motion *over* Σ_s; $V^{(s2)}$ is the sliding velocity of the shaper with respect to the face-gear. More details are given in Appendix B in reference 10.

The pointing of teeth (fig. 10) means that the tooth thickness on the top of the tooth becomes equal to zero. The location of the tooth pointing area may be determined by considering the intersection of the two opposite tooth surfaces at the top land of a tooth.

Computer programs for determination of limitations of the length of the face-gears have been developed at the University of Illinois at Chicago. A quick review of results obtained are represented in the following charts.

Figure 12 shows the minimum and maximum radius factors for the face-gear with various gear ratio m_{s2} and the pinion tooth numbers. In this example, the shaft angle is 80° and the pressure angle is 20°. The program is sufficiently general in that it has the ability to generate design charts over a wide range. Knowing the values of minimum and maximum radius factor we can obtain the values of L_1 and L_2 (fig. 13) by multiplying the radius factors by $N_2/2P$ where N_2 is the tooth number of the face-gear and P is the diametral pitch. For design convenience, a unitless design parameter $u_l = lP$ where $l = L_2 - L_1$ is usually considered. This parameter is similar to the parameter that express the ratio l/m where $m = 25.4/P$ is the module of spur or helical gears. The coefficient u_l depends on the number of teeth of the pinion and the gear ratio. The gear ratio must be $m_{12} > 3.8$ to obtain $u_l > 7$. The increase of the gear ratio reduces the dimensions of the fillet as shown in figure 14.

Computerized Simulation of Meshing and Contact of Pinion and Face-Gear

The bearing contact of pinion and face-gear tooth surfaces Σ_1 and Σ_2 is localized using the technique described in the previous section. Σ_1 and Σ_2 are in point contact at every instant. The computerized simulation of meshing and contact of Σ_1 and Σ_2 (Tooth Contact Analysis; TCA) can provide information on transmission errors and the shift of bearing contact that is caused by pinion-face-gear misalignment.

The idea of TCA is based on equations of tangency of contacting surfaces (fig. 15). Such equations express that the contacting surfaces Σ_1 and Σ_2 have, at any instant, a common position vector and collinear normals at their contact point M. For more details see reference 9 (and Appendix C in ref. 10).

Our investigation shows that the gear misalignment (change of the shaft angle, crossing of axes instead of intersection, axial displacement of face-gear) does not cause transmission errors. This is a great advantage of face-gear drives in comparison with spiral bevel gear drive.

However, gear misalignment does result in the shift of the contact path on the gear surfaces. The patterns of the bearing contact can be determined considering the motion of the instantaneous contact ellipse over the pinion-gear tooth surfaces in the process of meshing. The dimensions and orientation of the instantaneous contact ellipse can be found if the prinicpal directions

and curvatures of the contacting surfaces are determined at the current point of surface contact (ref. 9). The equations for computation of principal curvatures and directions are given in Appendix D in reference 10. The elastic approach of the surfaces is considered as known.

It is possible to control the location of the bearing contact by changing of the machine angle γ_m that is formed by the axes of the shaper and the face-gear. However, the small magnitude of $\Delta\gamma_m$ can be only implemented with a very precise control of γ_m. Figure 16 shows an example of the face-gear bearing contact prediction. The shift of bearing contact caused by gear misalignment and change in machine angle is given in reference 10.

Theoretical and Real Contact Ratio

The contact ratio m_c is determined with the equation

$$m_c = \frac{\phi_1^{(2)} - \phi_1^{(1)}}{\dfrac{360^\circ}{N_1}} \tag{8}$$

Here; $\phi_1^{(2)}$ and $\phi_1^{(1)}$ represent the angles of rotation of the pinion that correspond to the beginning and the end of meshing for one pair of teeth; N_1 is the number of pinion teeth. Angles $\phi_1^{(2)}$ and $\phi_1^{(1)}$ can be determined as the output data from the TCA computer program. The approximate value of $\Delta\phi = \phi_1^{(2)} - \phi_1^{(1)}$ can be determined from drawings of figure 10 that show the instantaneous contact lines referred to angles of pinion rotation. Taking into account that for drawings of figure 10 the stepsize of ϕ_1 is 3°, the number of contact lines that cover the surface of face-gear is 10, and $N_1 = 28$ (see table II), we obtain that the theoretical value of m_c is 2.33.

The localization of bearing contact is accompanied with the reduction of contact ratio, since the number of potential contact ellipses is reduced. Using an approach that is similar to the one discussed above, we have determined that $\left(\phi_1^{(2)} - \phi_1^{(1)}\right)$ is 20.8°, and the real contact ratio is 1.62.

Basic Ideas of Grinding

Two methods of grinding have been proposed: (1) the first one is based on simulation of generation of the face-gear by a shaper and (2) the second one is based on applicaton of a tool that is in quasi-line contact with the theoretical surface of the face-gear.

The basic prinicples of the first method are as follows: (1) the axial section of the grinding wheel is an involute curve (fig. 17), (2) the relative motion of the grinding wheel with respect to the face-gear is the same as the pinion and face-gear being in mesh, and (3) an additional motion of the grinding wheel, reciprocating translation that is parallel to the pinion axis, must be provided. The number of steps for the feeding motion (reciprocating translation) that corresponds to one cycle must be large enough to provide a smooth surface. (One cycle means the time that is required for grinding of one side surface of one tooth.) The deviations of ground surfaces from the theoretical ones for cases with 40 and 20 steps are shown in figure 18.

The second method for grinding is based on the following ideas: (1) the grinding wheel is a cone or a surface of revolution, (2) the cone is in continuous tangency with the theoretical surface of the face-gear at any point of the chosen mean line of the theoretical surface, (3) the cone moves along the mean line and changes its orientation (fig. 19), and (4) the installment of the cone at any moment must be determined in accordance with the curvatures of the face-gear. The deviations of ground surface from the theoretical one by this method are shown in figure 20.

Both of the methods of grinding can be performed using a six-degree-of-freedom machine that is numerically controlled.

EXPERIMENTAL TESTS

Experimental tests on face-gears were performed in the NASA Lewis spiral bevel gear rig (ref. 11). The face-gears tested (fig. 21) were basically a half-size version of the MDHC/Lucas ART design. The gears were 16 pitch with 28 teeth on the pinion and 107 on the face-gear. The shaft angle was 90° to accommodate the rig. The gears were made of Maraging 300 steel per AMS 6514. The pinions were nitrided and ground with a case hardness of R_c 58. The face-gears were shaper cut and hardened to R_c 52. For the tests, 100-percent test torque was defined as 68 N•m (600 in.•lb) pinion torque for a power of 135 kW (180 hp) at 19 000 rpm pinion speed. The test torque provided slightly increased bending and compressive stresses when compared to the full scale design.

The NASA Lewis spiral bevel gear rig (fig. 22) operates on a closed loop or torque-regenerative principle. Two sets of pinion/face-gears are used in the loop with the two pinions connected by a cross shaft. The outputs of the two face-gears are connected through a helical gear mesh. A hydraulic loading system is connected to the helical mesh which puts a thrust load on the mesh, and thus, the torque in the loop. A variable speed motor is connected by a belt to the loop and powers the test stand.

A limited amount of test gears were available for test (four pinions and four face-gears). The objective of the tests were to demonstrate the feasibility of face-gears and determine the failure modes for high power applications. Four sets of gears successfully completed 26-hr (30×10^6 pinion cycles) endurance runs at 100-percent speed and torque. The gears were run at 74 °C (165 °F) oil inlet temperature using an ample supply of DOD–L–85734 lubricant at approximately 0.8 gpm per mesh.

The contact pattern on the teeth was good and developed on the full tooth of the face-gear. The pinion teeth showed only minimal change from their original manufactured condition. The face-gear teeth, however, had some surface distress. The teeth from the test side (pinion driving the face-gear) were generally in good condition except for small areas of micro-pitting randomly scattered over the active profile. The teeth from the slave side (face-gear driving the pinion) had small pit lines in some instances in the middle region of the teeth along with micro-pitting in the root area of the active profile.

The gears were subsequently run at 200-percent torque and 100-percent speed. The first test (two sets of gears) lasted the 26 hr. The pinions and the test-side face-gears showed slightly increased wear but were generally in good shape. The slave-side face-gear surface distress became more pronounced. The second test (the additional two sets of gears) was suspended after about 10.5 hr due to a tooth breakage on one of the face-gears (slave side). The breakage originated from the surface pit line from the previous test. The remaining components looked basically the same as in the 100-percent torque tests.

The results, although limited, demonstrated the feasibility of face-gears in high-speed, high-load applications. The tests did show surface distress with the face-gears, however. The use of a hardened, ground gear steel (in use for conventional aircraft gears today but not presently available for face-gears) would significantly increase the surface durability and make face-gears available for high-power application.

CONCLUSION

The use of face-gears in helicopter transmissions was explored. A lightweight, split-torque transmission design utilizing face-gears was described. Face-gear design and geometry were investigated. Topics included tooth generation, minimum inner and maximum outer radii, tooth contact analysis, contact ratio, gear eccentricity, grinding, and structural stiffness. Face-gear experimental studies were also included. The following results were obtained:

1. The feasibility of face-gears in high-speed, high-load applications such as helicopter transmissions was demonstrated through experimental testing. Face-gears which were basically a half-scale version of the MDHC/Lucas ART design were tested in the NASA Lewis spiral bevel rig. The pinions and the gears showed good contact patterns and ran at 100- and 200-percent design torque. However, the face-gears did have some surface distress.

2. Analytical studies of transmission errors showed that the face-gear drive is relatively insensitive to gear misalignment. Tooth contact, however, is affected by misalignment resulting in a shift of the contact on the tooth surfaces. A method of localizing contact by changing tool settings of the generating machine was explored.

3. The length of the face-gear tooth was limited due to possible undercutting by the shaper in the dedendum area and pointing of the teeth in the addendum area. Design charts were developed to determine minimum inner and maximum outer radii.

4. The hardened tooth surface can be ground with acceptable deviations by two methods. One of these methods need application of a six-degree-of-freedom machine. One of the six degrees of freedom is required to rotate the grinding cone for speed of manufacture.

5. A finite element analysis of the pinion and face-gear structure in a split-torque design provided data on load sharing. Among the cases studied, an even torque split was provided when the stiffness of the pinion shaft front support (close to the face-gear mesh) was about an order of magnitude less than a typical bearing support.

ACKNOWLEDGMENTS

The authors express their gratitude to Mr. Luis Bohorquez and Mr. R.J. King (McDonnell Douglas Helicopter Co.) and Mr. Robert Handschuh (U.S. Army Propulsion Directorate, NASA Lewis) for their invaluable support of this research project.

REFERENCES

1. Bill, R.C.: Advanced Rotorcraft Transmission Program. NASA TM–103276, 1990.

2. Bossler, R.B.; and Heath, G.F.: Advanced Rotorcraft Transmission (ART) Program Status. Rotary Wing Propulsion Specialists' Meeting, Proceedings, American Helicopter Society, Alexandria, VA, 1990, p. 8.

3. Bossler, R.B.; and Heath, G.F.: Advanced Rotorcraft Transmission (ART) Program Status. AIAA Paper 91–1906, 1991.

4. Buckingham, E.: Analytical Mechanics of Gears. Dover Publications, New York, 1949.

5. Dudley, D.W.: Gear Handbook. McGraw-Hill Book Co., New York, 1962.

6. Davidov, J.S.: Noninvolute Gearing (in Russian), Mashgiz, Moscow, USSR, 1950.

7. Litvin, F.L.: Theory of Gearing (in Russian), Second ed., Nauka, Moscow, USSR, 1968.

8. Litvin, F.L., et al.: Application of Face-Gear Drives in Helicopter Transmissions. NASA TM–105655, 1992.

9. Litvin, F.L., Theory of Gearing. NASA RP–1212, 1989.

10. Litvin, F.L., et al.: Design and Geometry of Face-Gear Drives. To be published in J. of Mech. Des.

11. Handschuh, R.F.; Lewicki, D.G.; and Bossler, R.: Experimental Testing of Prototype Face-Gears for Helicopter Transmissions. NASA TM-105434, 1992.

TABLE I. – ADVANCED ROTORCRAFT TRANSMISSION TORQUE SPLITTING PERCENTAGES

Case number	Support of pinion shaft		Gear meshing clearance (inch) due to backlash adjustment		Split torque percentage, percent	
	Front-end spring rate, lb/in.	Rear-end spring rate, lb/in.	Face-down gear	Face-up gear	Face-down gear	Face-up gear
1	K=0 (free float)	K=∞ (restrained)	0	0	51.58	48.42
2	K=∞ (restrained)	K=∞ (restrained)	0	0	56.87	43.13
3	[a]$K=6.0\times10^5$	[a]$K=6.0\times10^5$	0	0	53.11	46.89
4	$K=6.0\times10^4$	$K=6.0\times10^5$	0	0	51.41	48.59
5	$K=6.0\times10^4$	$K=6.0\times10^5$	0	.0005	51.55	48.45
6	$K=6.0\times10^4$	$K=6.0\times10^5$	0	.005	52.86	47.14
7	K=∞	$K=6.0\times10^5$	0	.005	81.66	18.34
8	$K=6.0\times10^4$	$K=6.0\times10^5$	.003	0	50.54	49.46
9	$K=6.0\times10^4$	$K=6.0\times10^5$	.005	0	49.97	50.03

[a]6.0×10^5 lb/in. is the translational spring rate for typical bearing and housing support in helicopter transmissions.

TABLE II. – INPUT FACE-GEAR DRIVE DESIGN DATA

Design parameter	Input data
Shaft angle	80°
Pinion number of teeth	28
Gear number of teeth	107
Diametral pitch	8
Pressure angle	25°

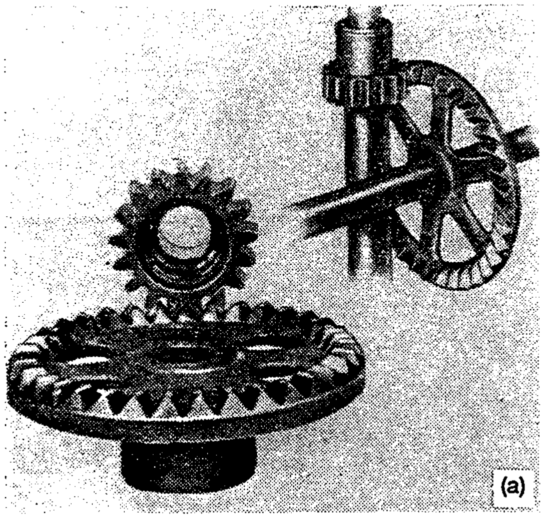

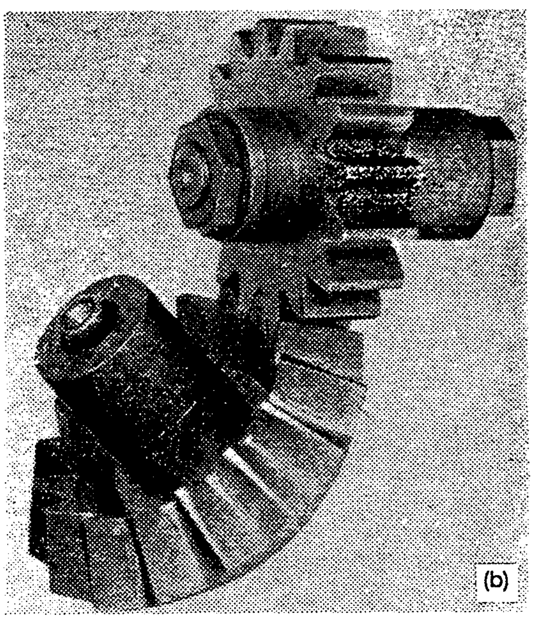

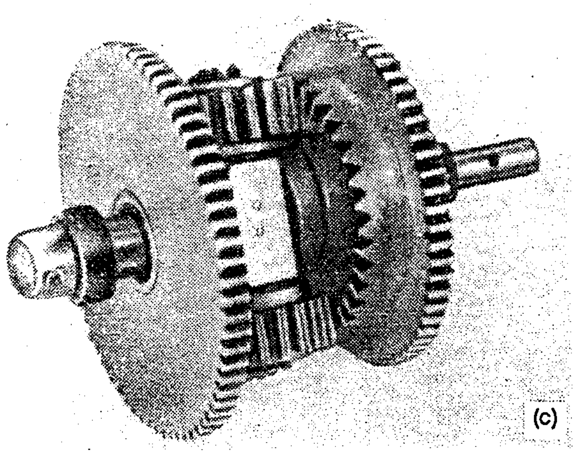

Figure 1.—Examples of the application of face-gear drives.

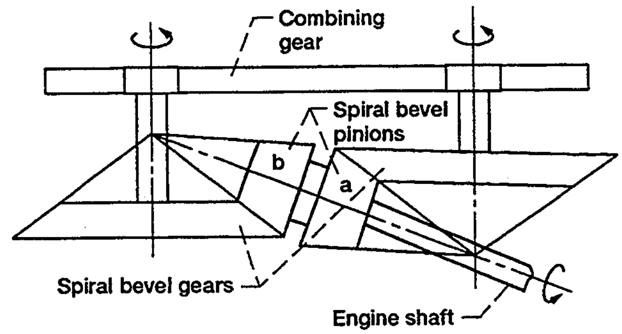

(a) Bevel gear arrangement.

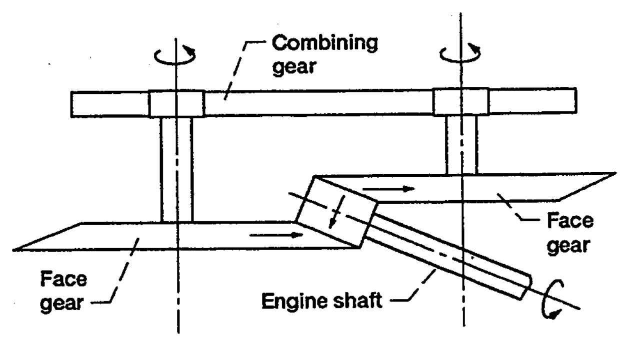

(b) Face-gear arrangement.

Figure 2.—Different versions of split-torque.

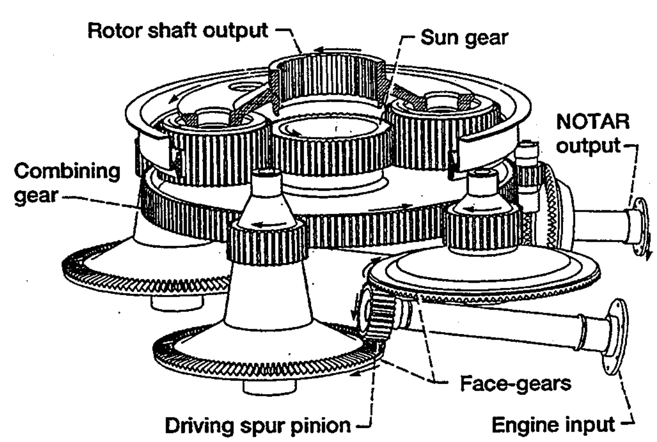

Figure 3.—Three-stage split-torque single planetary transmission.

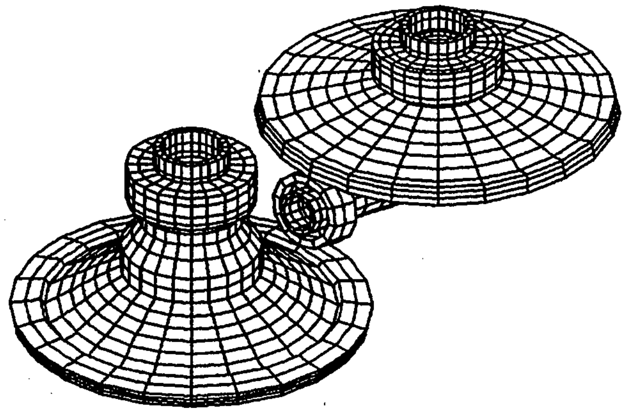

Figure 4.—Finite element model of the split-torque drive.

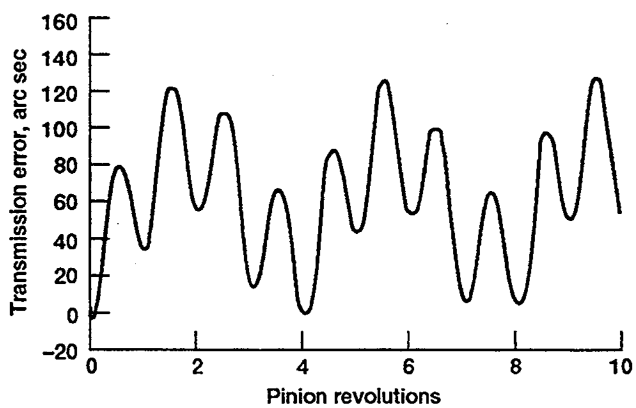

Figure 5.—Typical transmission errors for a face gear mesh.

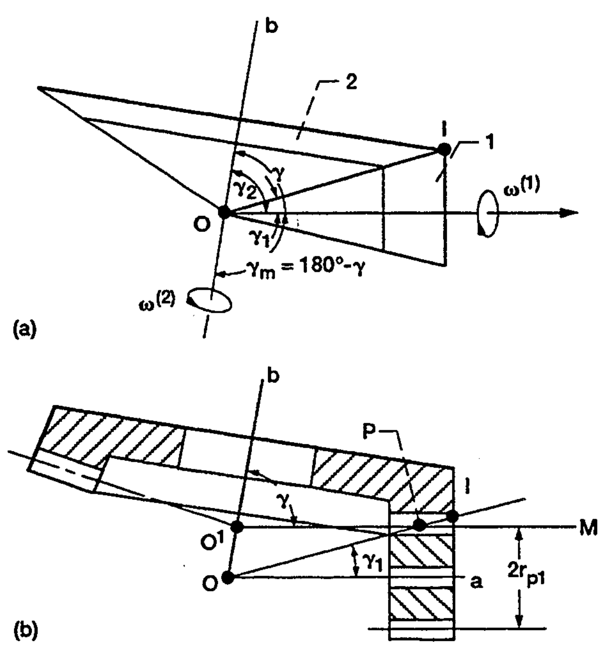

Figure 6.—Pitch surfaces.

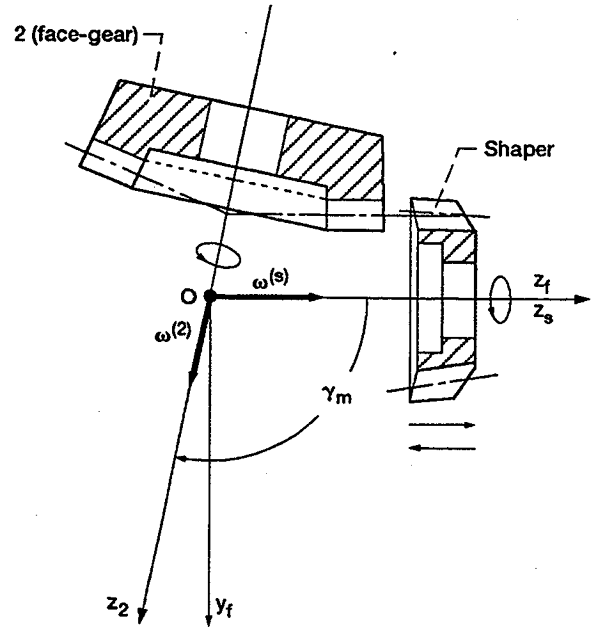

Figure 7.—Face-gear generation.

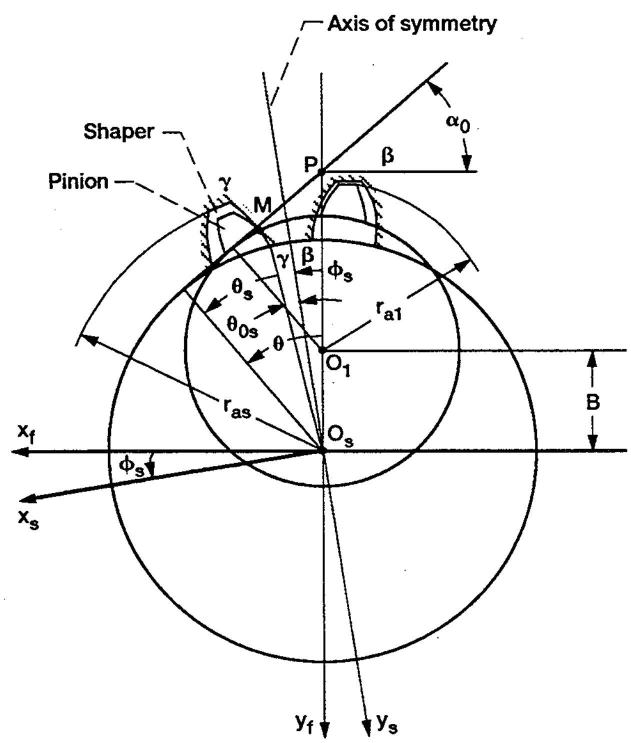

Figure 8.—Imaginary tangency of shaper and pinion surfaces.

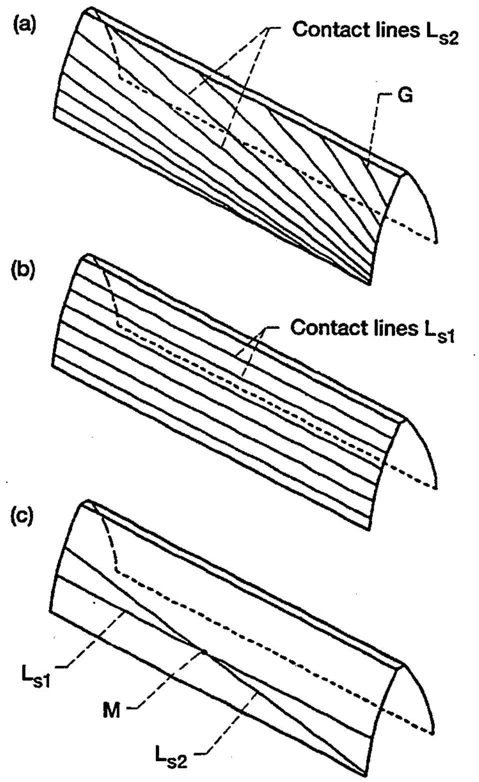

Figure 9.—Contact lines on shaper tooth surface.

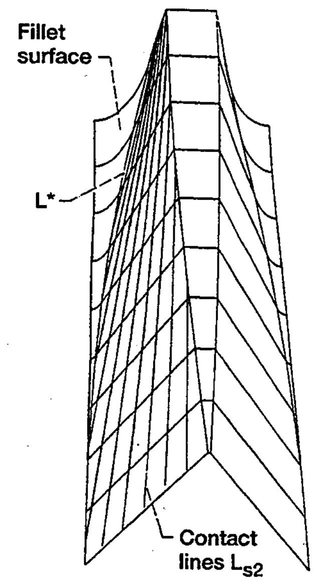

Figure 10.—Contact lines on face-gear tooth surface.

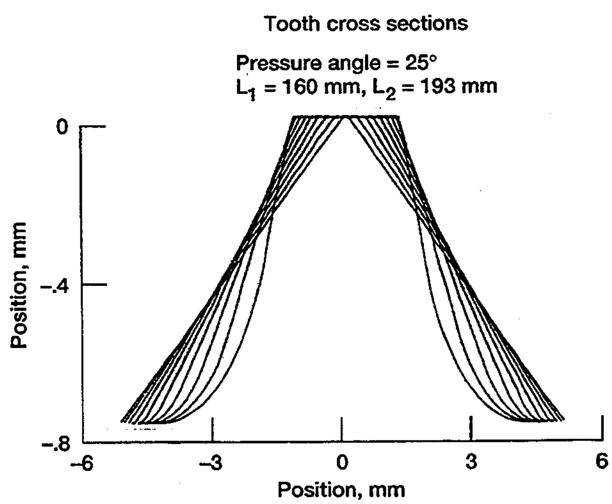

Figure 11.—Cross-sections of face-gear tooth surface.

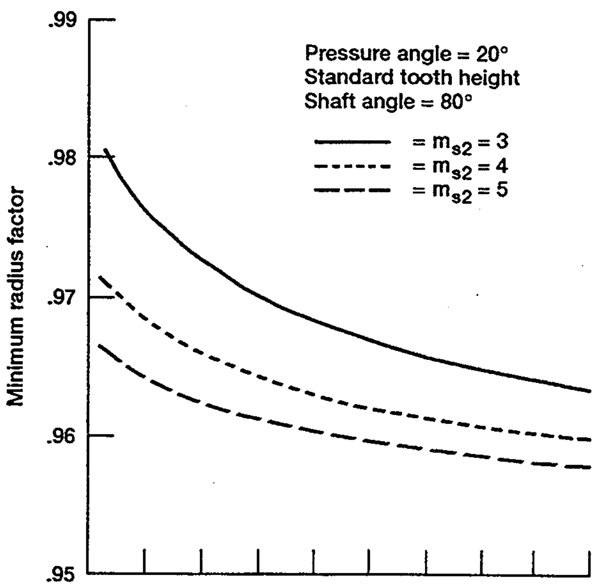

(a) Minimum radius factor.

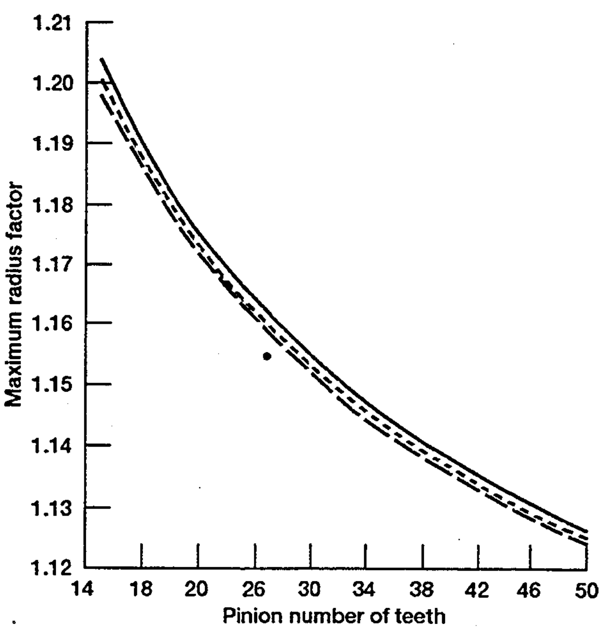

(b) Maximum radius factor.

Figure 12.—Face-gear minimum and maximum radius factors.

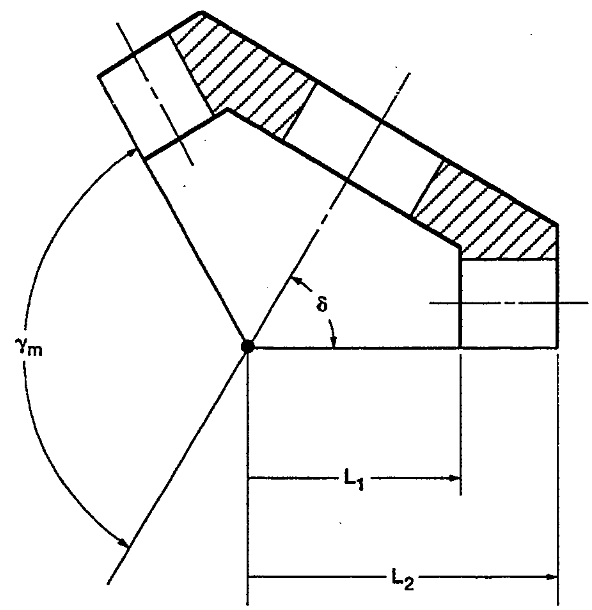

Figure 13.—The determination of face-gear tooth length.

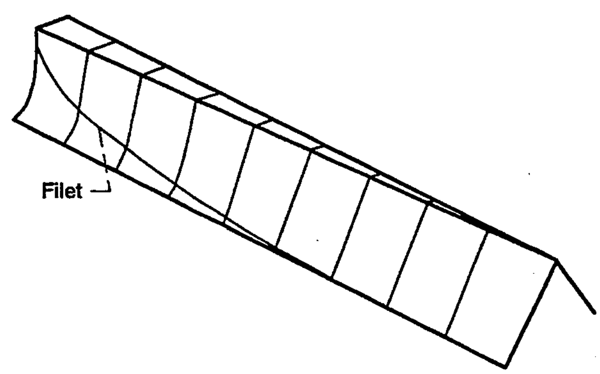

$N_s = 31$, $N_1 = 28$, $N_2 = 140$, $m_{12} = 5$, $u_t = 10.14$

Figure 14.—Modified face-gear tooth.

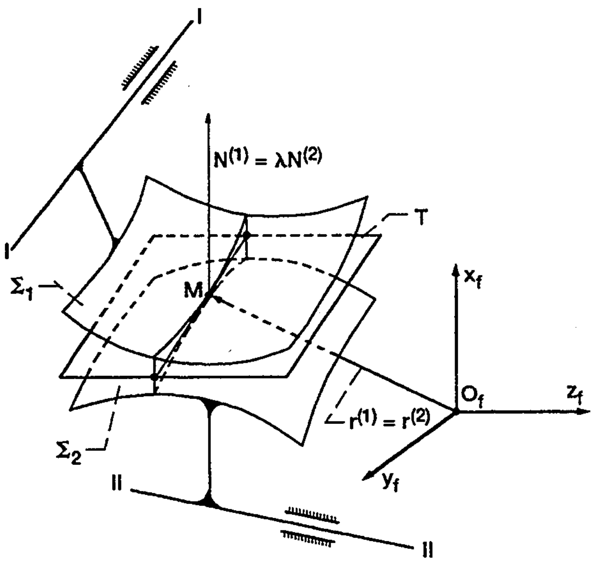

Figure 15.—Contact of mating surfaces.

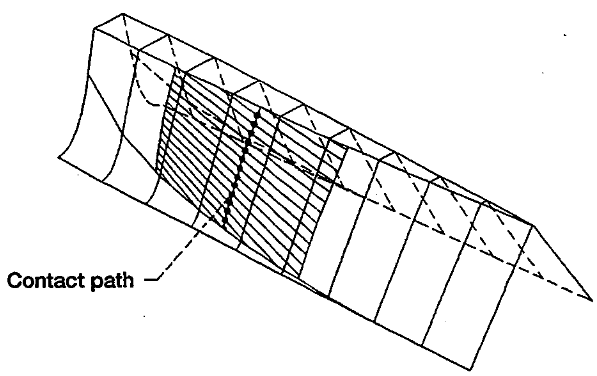

Figure 16.—Aligned face-gear drive: localized bearing contact with $\Delta N = 3$.

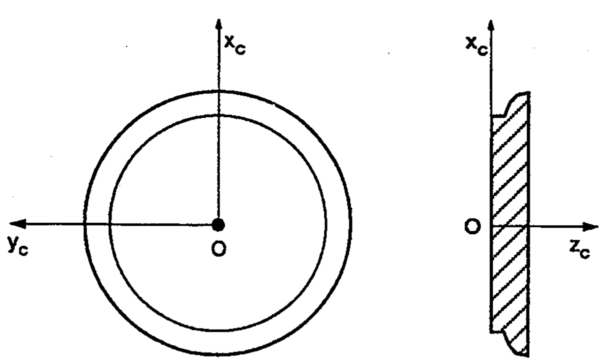

Figure 17.—Installment of the grinding wheel (first method).

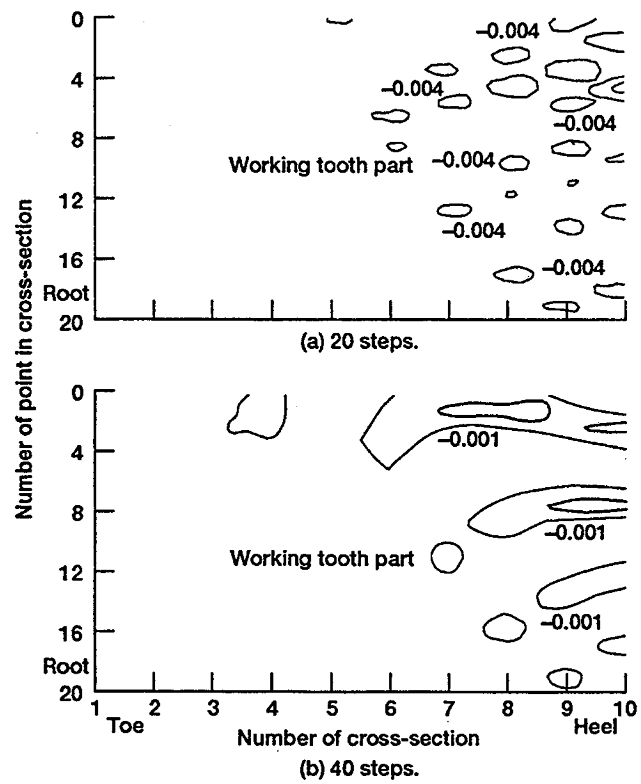

Figure 18.—Deviations of ground surface from theoretical one (first method) (deviations in mm).

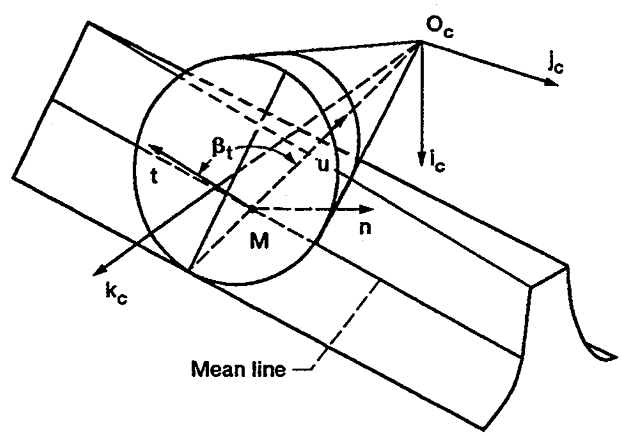

Figure 19.—Installment of the grinding wheel (second method).

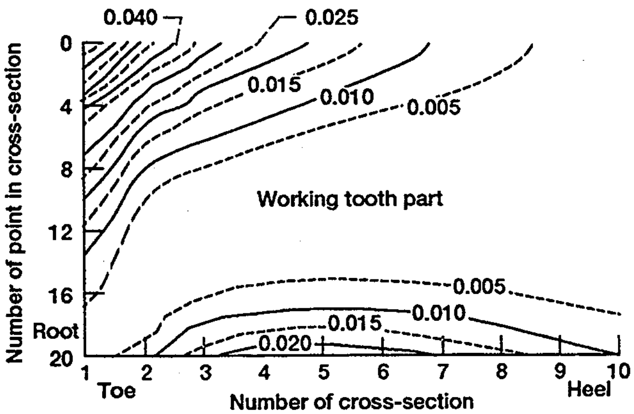

Figure 20.—Deviations of ground surface from theoretical one (second method) (deviations in mm).

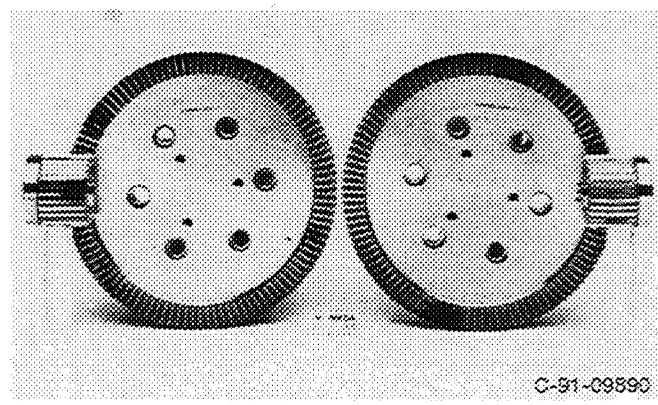

Figure 21.—Test gears.

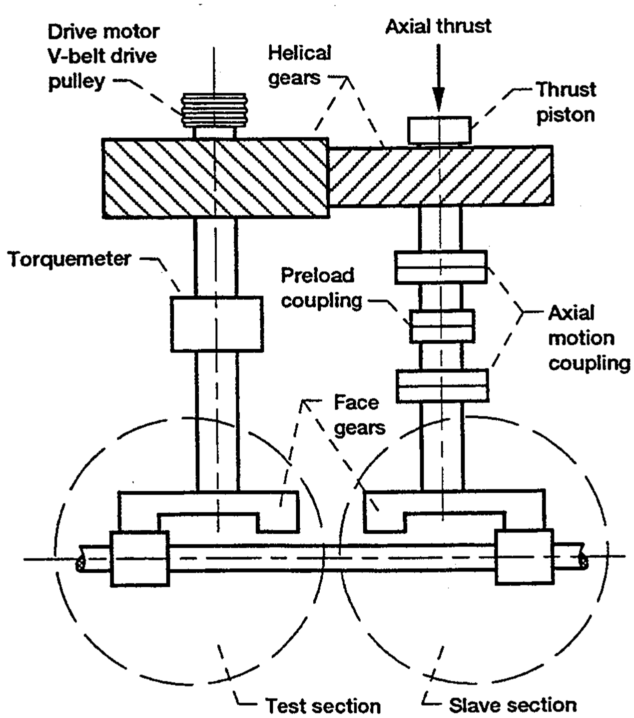

Figure 22.—Crossectional view of facility (face-gears installed).

REPORT DOCUMENTATION PAGE

Form Approved
OMB No. 0704-0188

1. AGENCY USE ONLY *(Leave blank)*	2. REPORT DATE	3. REPORT TYPE AND DATES COVERED
	October 1992	Technical Memorandum

4. TITLE AND SUBTITLE

Face-Gear Drives: Design, Analysis, and Testing
for Helicopter Transmission Applications

5. FUNDING NUMBERS

WU–505–63–36
1L162211A47A

6. AUTHOR(S)

F.L. Litvin, J.-C. Wang, R.B. Bossler, Jr., Y.-J.D. Chen,
G. Heath, and D.G. Lewicki

7. PERFORMING ORGANIZATION NAME(S) AND ADDRESS(ES)

NASA Lewis Research Center
Cleveland, Ohio 44135–3191
and
Propulsion Directorate
U.S. Army Aviation Systems Command
Cleveland, Ohio 44135–3191

8. PERFORMING ORGANIZATION REPORT NUMBER

E-7743

9. SPONSORING/MONITORING AGENCY NAMES(S) AND ADDRESS(ES)

National Aeronautics and Space Administration
Washington, D.C. 20546–0001
and
U.S. Army Aviation Systems Command
St. Louis, Mo. 63120–1798

10. SPONSORING/MONITORING AGENCY REPORT NUMBER

NASA TM-106101
AVSCOM TR92–C–009

11. SUPPLEMENTARY NOTES

Prepared for the AGMA 1992 Fall Technical Meeting, sponsored by American Gear Manufacturers Association, Baltimore, Maryland, October 26-28, 1992. F.L. Litvin and J.-C. Wang, University of Illinois at Chicago, Chicago, Illinois, 60680, R.B. Bossler, Jr. Lucas Western, Inc. City of Industry, California, 91749, Y.-J.D. Chen and G. Heath, McDonnell Douglas Helicopter Co., Mesa, Arizona, 85205, and D.G. Lewicki, Propulsion Directorate, U.S. Army Aviation Systems Command. Responsible person, David G. Lewicki, (216) 433-3970.

12a. DISTRIBUTION/AVAILABILITY STATEMENT	12b. DISTRIBUTION CODE
Unclassified - Unlimited Subject Category 37	

13. ABSTRACT ***(Maximum 200 words)***

The use of face-gears in helicopter transmissions was explored. A light-weight, split-torque transmission design utilizing face-gears is described. Face-gear design and geometry were investigated. Topics included tooth generation, limiting inner and outer radii, tooth contact analysis, contact ratio, gear eccentricity, grinding, and structural stiffness. Design charts were developed to determine minimum and maximum face-gear inner and outer radii. An analytical study showed that the face-gear drive is relatively insensitive to gear misalignment with respect to transmission errors, but the tooth contact is affected by misalignment. A method of localizing the bearing contact to permit operation with misalignment was explored. Two new methods for grinding of the face-gear tooth surfaces were also investigated. The proper choice of shaft stiffness enabled good load sharing in the split-torque transmission design. Face-gear experimental studies were also conducted. These tests demonstrated the feasibility of face-gears in high-speed, high-load applications such as helicopter transmissions.

14. SUBJECT TERMS	15. NUMBER OF PAGES
Transmissions (machine elements); Gears; Design; Helicopters	16
	16. PRICE CODE
	A03

17. SECURITY CLASSIFICATION OF REPORT	18. SECURITY CLASSIFICATION OF THIS PAGE	19. SECURITY CLASSIFICATION OF ABSTRACT	20. LIMITATION OF ABSTRACT
Unclassified	Unclassified	Unclassified	